Cancer Research

SHMT2 Desuccinylation by SIRT5 Drives Cancer Cell Proliferation

Xin Yang[1], Zhe Wang[1], Xin Li[2], Boya Liu[1], Minghui Liu[1], Lu Liu[1], Shuaiyi Chen[1], Mengmeng Ren[1], Yankun Wang[1], Miao Yu[1], Bo Wang[3], Junhua Zou[1], Wei-Guo Zhu[4], Yuxin Yin[5], Wei Gu[6], and Jianyuan Luo[1,7]

Abstract

The mitochondrial serine hydroxymethyltransferase SHMT2, which catalyzes the rate-limiting step in serine catabolism, drives cancer cell proliferation, but how this role is regulated is undefined. Here, we report that the sirtuin SIRT5 desuccinylates SHMT2 to increase its activity and drive serine catabolism in tumor cells. SIRT5 interaction directly mediated desuccinylation of lysine 280 on SHMT2, which was crucial for activating its enzymatic activity. Conversely, hypersuccinylation of SHMT2 at lysine 280 was sufficient to inhibit its enzymatic activity and downregulate tumor cell growth *in vitro* and *in vivo*. Notably, SIRT5 inactivation led to SHMT2 enzymatic downregulation and to abrogated cell growth under metabolic stress. Our results reveal that SHMT2 desuccinylation is a pivotal signal in cancer cells to adapt serine metabolic processes for rapid growth, and they highlight SIRT5 as a candidate target for suppressing serine catabolism as a strategy to block tumor growth.

Significance: These findings reveal a novel mechanism for controlling cancer cell proliferation by blocking serine catabolism, as a general strategy to impede tumor growth. *Cancer Res; 78(2); 372–86.* *©2017 AACR.*

Introduction

Mitochondrial serine hydroxymethyltransferase (SHMT2), a pyridoxal phosphate (PLP) binding protein, catalyzes the cleavage of serine to glycine accompanied with the production of 5, 10-methylenetetrahydrofolate (5, 10-CH_2-THF), which is an essential intermediate for purine biosynthesis (1–3). SHMT2 is a direct c-myc target gene for cell survival during hypoxia (4, 5), and its expression drives glioma cell survival in ischemia (6). *De novo* thymidylate synthesis by SHMT2 in the mitochondrial matrix protects mitochondrial DNA (mtDNA) from uracil accumulation (7).

SHMT2 plays a regulatory role as the bridge for exchange between serine catabolism and one-carbon metabolism, and the small molecular metabolite among them controls cell proliferation and redox homeostasis significantly. At first, glycine consumption is regarded as a key factor for rapid cell proliferation (8). Further study suggests that serine demonstrates stronger functionality than glycine in nucleotide biosynthesis and tumor growth (9). Serine is also the only amino acid that functions as the activator of pyruvate kinase isoform M2 (PKM2). Thus, serine deprivation can reduce PKM2 activity, which is also in agreement with limiting PKM2 activity and reducing oxygen consumption by SHMT2 overexpression (6, 10, 11). Serine-driven one-carbon metabolism is identified as an important pathway for NADPH generation (12, 13). Serine starvation leads to the increasing of AMP, the decreasing of ATP, and a different state of DNA/RNA methylation (14).

Several factors control serine biosynthesis and one-carbon metabolism: NRF2 or mTORC1 signaling pathway or G9A epigenetically activates these enzymes through transcriptional regulation (15–17). In addition, TP53 promotes metabolic remodeling under serine starvation for cell proliferation (18, 19). MDM2 also regulates serine metabolism during oxidative stress independent of p53 (20). However, the mechanism of SHMT2 regulated by posttranslational modification (PTM) remains unknown.

SIRT5 is defined as a NAD^+-dependent lysine deacetylase, demalonylase, desuccinylase, and deglutarylase (21), which regulates several cellular metabolism pathways, including ammonia metabolism, fatty acid oxidation, and glycolysis. It targets carbamoyl phosphate synthetase 1 (CPS1), urate oxidase (UOX), and glutaminase (GLS) to regulate the balance of the urea cycle and mitophagy (22–25). It controls fatty acid oxidation through desuccinylating 3-hydroxy-3-methylglutaryl-CoA synthase 2 (HMGCS2), enoyl-CoA hydratase α-subunit (ECHA), and demalonylating malonyl-CoA decarboxylase (26–28). It also functions in glycolysis and TCA cycle by controlling the PTM level of succinate dehydrogenase complex (GDH), pyruvate dehydrogenase complex (PDH), and GAPDH (29, 30). In response to oxidative stress, SIRT5 desuccinylates superoxide dismutase [Cu-Zn] (SOD1), isocitrate dehydrogenase 2 (IDH2), and deglutarylates glucose-6-phosphate 1-dehydrogenase (G6PD) to maintain cellular redox homeostasis (31, 32). SIRT5 may play a role in tumorigenesis. However, the precise mechanism remains elusive as SIRT5 could function as an oncogene or tumor suppressor depending on its targets (33, 34).

[1]Department of Medical Genetics, Peking University Health Science Center, Beijing, China. [2]Department of Biotechnology and Biomedicine, Technical University of Denmark, Lyngby, Denmark. [3]Department of Gastroenterological Surgery, Peking University People's Hospital, Beijing, China. [4]Department of Biochemistry and Molecular Biology, Shenzhen University School of Medicine, Shenzhen, China. [5]Institute of Systems Biomedicine, Peking University Health Science Center, Beijing, China. [6]Institute for Cancer Genetics, Columbia University, New York, New York. [7]Department of Medical & Research Technology, School of Medicine, University of Maryland, Baltimore, Maryland.

Note: Supplementary data for this article are available at Cancer Research Online (http://cancerres.aacrjournals.org/).

Corresponding Author: Jianyuan Luo, Department of Medical Genetics, Peking University, 38 Xueyuan Road, Beijing 100191, China. Phone: 8610-8280-5861; Fax: 8610-6201-5582; Email: luojianyuan@bjmu.edu.cn

doi: 10.1158/0008-5472.CAN-17-1912

In this study, we purified a SIRT5 complex in cells and identified the network of SIRT5 targets with mass spectrometry. We found that SIRT5 participates in serine catabolism for cell proliferation. We identified SHMT2 as the desuccinylation substrate of SIRT5. Under metabolic stress, SIRT5 directly interacts with and desuccinylates SHMT2 at lysine 280 to activate its enzymatic activity for regulation of tumor cell growth. Our results on the SIRT5 targeting network and its regulation of SHMT2 provide new insight on mitochondrial sirtuins' functions in the regulation of cancer cell metabolism.

Materials and Methods

Cell culture and treatment

HEK293T, HCT116 ($p53^{+/+}$), and U2OS cells were obtained from ATCC between 2012 and 2016 and maintained at 37°C and 5% CO_2 in DMEM (Invitrogen) supplemented with 10% (v/v) FBS, 100 U/mL penicillin, and 100 μg/mL streptomycin (Sigma-Aldrich). All cell lines were tested for mycoplasma contamination and authenticated utilizing short tandem repeat profiling. The same batch of cells was thawed every 1 to 2 months. For serine/glycine, aspartate/asparagine, or glucose starvation treatment, cells were washed by PBS for twice and fed with none serine/glycine medium (-SG), none aspartate/asparagine medium, or none glucose medium, respectively. When cells were under metabolic starvation, the medium was changed every 12 hours. None serine/glycine medium contains minimum Eagle medium (11095, Invitrogen), 1 × MEM Vitamin Solution (100×; 11120, Invitrogen), 17 mmol/L α-D-glucose (158968, Sigma-Aldrich), and 10% dialyzed FBS (26400, Invitrogen). For normal serine/glycine medium, 0.4 mmol/L serine (S4311, Sigma-Aldrich) and 0.4 mmol/L glycine (G8790, Sigma-Aldrich) were added back to none serine/glycine medium (+SG). For normal aspartate/asparagine medium, 0.15 mmol/L aspartate (A7219, Sigma-Aldrich) and 0.4 mmol/L asparagine (A4159, Sigma-Aldrich) were added back to none aspartate/ asparagine medium. Nicotinamide, sodium butyrate (NaBu), menadione, formate, glutathione (GSH), N-acetylcysteine (NAC), and dimethyl 3-hydroxyglutarate (DMHG) treatment is described in figure legends.

CRISPR-Cas9 knockout and rescued cell lines

To generate U2OS SIRT5, U2OS SHMT2, or HCT116 SHMT2 knockout (KO; down) cell lines, sgRNA sequences were ligased into LentiCRISPRv2 plasmid and then cotransfected with viral packaging plasmids (psPAX2 and pMD2G) into HEK293T cells. Six hours after transfection, medium was changed, and viral supernatant was filtered through 0.45-μm strainer 42 hours later. Targeted cells were infected by viral supernatant and selected by 1 μg/mL puromycin for 2 weeks. The sgRNA sequences targeting SHMT2 and SIRT5 were designed by CRISPR designer at http://crispr.mit.edu/. The guide sequences targeting Exon 4 of human SHMT2 and Exon 3 of human SIRT5 are shown.

SHMT2: 5′-CAACCTCACGACCGGATCAT-3′
SIRT5: 5′-GTTCTACCACTACCGGCGGG-3′

For SHMT2-rescued cell lines, cDNA of Flag-tagged SHMT2 wild type (WT) and SHMT2 K280E mutant was subcloned into pQCXIH retrovirus vector. The two plasmids were cotransfected with viral packaging plasmids (*vsvg* and *gag*) into HEK293T cells, respectively. Twenty-four hours after transfection, viral supernatant was filtered and infected into U2OS or HCT116 SHMT2 KO cell line. The infected cells were selected by 150 μg/mL hygromycin for 2 weeks.

Plasmids

cDNA of SIRT3, SIRT4, SIRT5, SIRT5Δ50, CS, PKM2, SLC25A13, HSD17B10, and SHMT2 was amplified and cloned into pcDNA3.1 vector. SIRT5- and SHMT2-mutant constructs were generated with KOD Plus Mutagenesis Kit (TOYOBO). MTHFD2 and SIRT5 full-length cDNA was subcloned into pGEX 4T-3 vector. All expression constructs were checked by Sanger sequencing.

Western blotting and antibodies

Proteins were analyzed by Western blotting according to the standard methods. Visualization was performed using ECL (Thermo Fisher Scientific, #32106). The antibodies used were commercially obtained: anti-Flag-tag (Sigma-Aldrich, F-3165, with 1:10,000 dilution), anti–γ-tubulin (Sigma-Aldrich, T6557, with 1:5,000 dilution); anti-PKM2 (Cell Signaling Technology, #4053, with 1:10,000 dilution), anti-VDAC (Cell Signaling Technology, #4661, with 1:1,000 dilution), anti-SHMT2 (Cell Signaling Technology, #12762, with 1:1,000 dilution), anti-SIRT5 (Cell Signaling Technology, #8782, with 1:1,000 dilution), anti–pan-acetyllysine (Cell Signaling Technology, #9441L, with 1:1,000 dilution), anti-S6 (Cell Signaling Technology, #2217, with 1:1,000 dilution), anti-phospho-S6 (Ser235/236; Cell Signaling Technology, #4858, with 1:1,000 dilution); anti-SHMT2 (Santa Cruz Biotechnology, sc-390641, with 1:500 dilution), anti–β-actin (Santa Cruz Biotechnology, sc-47778, with 1:10,000 dilution); anti-SIRT5 (R&D, AF5914, for coimmunoprecipitation assay); anti-pan-glutaryllysine (PTM, #1151, with 1:500 dilution), anti–pan-succinyllysine (PTM, #419, with 1:1,000 dilution), and anti–HA-tag (Pierce, #26183, with 1:5,000 dilution).

qRT-PCR

Total RNA was extracted using TRIzol reagent (Sigma), and RNA was reverse transcribed into cDNA by qPCR RT Kit (FSQ-101 TOYOBO). Quantitative PCR was performed using 7500 Fast Real-time PCR System (Applied Biosystems) with qPCR SYBR Green Master Mix (Q131-03 Vazyme). The quantity mRNA was calculated using the method $\Delta\Delta C_t$ and normalized to actin. The real-time PCR primers are as listed below:

Sirt5 Fwd: 5′-TGGCTCGGCCAAGTTCAAGTATG-3′
Sirt5 Rev: 5′-AAGGTCGGAACACCACTTTCTGC-3′
Actin Fwd: 5′-TCCATCATGAAGTGTGACG-3′
Actin Rev: 5′-TACTCCTGCTTGCTGATCCAC-3′

Coimmunoprecipitation

Total cells were lysed in BC100 buffer [20 mmol/L Tris-HCl (pH 7.9), 100 mmol/L NaCl, 0.2% NP-40, and 20% glycerol] containing protease inhibitor cocktail (Sigma-Aldrich), 1 mmol/L dithiothreitol and 1 mmol/L phenylmethyl sulfonyl fluoride (Sigma-Aldrich). Whole lysates were incubated with 1 μg of mouse anti-SHMT2 or sheep anti-SIRT5 as described previously (35). Briefly, bounded proteins were eluted with 0.1 mol/L glycine (pH 2.5) and then neutralized with 1 mol/L Tris buffer to prevent disturbance of heavy chain (around 55 kDa). The elution was analyzed by Western blot analysis.

Mitochondria extraction and SIRT5 complex

Mitochondria extraction was performed, and crude mitochondria was used for SIRT5 natural complex purification (36). In briefly, crude mitochondria was lysed by BC100 buffer and filtered by 0.45-μm filter. Mitochondrial lysates were incubated with M2 beads overnight and eluted by Flag peptides (Sigma). Total elution was subjected to SDS-PAGE and stained by Coomassie blue. The unique protein bands and total elution were tryptic digested and analyzed by mass spectrometry.

Immunoprecipitation and protein purification

Total cells were lysed in Flag lysis buffer [50 mmol/L Tris-HCl (pH 7.9), 137 mmol/L NaCl, 1% Triton X-100, 0.2% Sarkosyl, 1 mmol/L NaF, 1 mmol/L Na_3VO_4, and 10% glycerol] containing protease inhibitor cocktail, 1 mmol/L dithiothreitol, and 1 mmol/L phenylmethyl sulfonyl fluoride. Immunoprecipitation were carried out by incubating with M2 Affinity gel (Sigma-Aldrich) for over 4 hours at 4°C. After the incubation, beads were washed for four times with ice-cold BC100 buffer and eluted by Flag peptides. GST-MTHFD2 were expressed and purified from Rosetta bacterial cells and bound to a GST-agarose column (Novagen). After the incubation, beads were eluted by GSH and diluted by 4 volumes of BC100 buffer rapidly.

Identification of SHMT2 PTM sites

HEK293T cells were transfected with SHMT2-Flag plasmids and untreated or treated with 10 mmol/L NAM and 1 μmol/L TSA for 6 hours before harvest. Cells were lysed by Flag lysis buffer plus 10 mmol/L NAM and 1 μmol/L TSA, and cell lysate was immunoprecipitated with M2 beads overnight. Immunoprecipitated SHMT2 proteins were subjected to 8% SDS-PAGE gel, and SHMT2 bands were excised from the gel and analyzed by mass spectrometry. Distinct modification sites were chosen for further potential succinylation sites analysis.

In vitro succinylation assay

Reactions contain succinylation buffer [20 mmol/L pH 8.0 HEPES, 1 mmol/L dithiothreitol, 1 mmol/L phenylmethyl sulfonyl fluoride, and 0.1 mg/mL BSA], purified SHMT2 proteins, and different concentrations of succinyl-CoA (S1129, Sigma-Aldrich). Reaction mixture was incubated at 30°C for 15 minutes. The reaction was stopped by adding loading buffer and subjected to SDS-PAGE. Proteins were analyzed by Western blot analysis and Coomassie blue or Ponceau S.

In vitro desuccinylation assay

Hypersuccinylated SHMT2 proteins purified from HEK293T cells were incubated with purified SIRT3, SIRT5, or SIRT5-H158Y in the presence or absence of 1 mmol/L NAD^+ at 30°C for 1 hour with desuccinylation buffer [50 mmol/L Tris-HCl (pH 8.0), 100 mmol/L NaCl, 8 mmol/L $MgCl_2$, 20% glycerol, 1 mmol/L dithiothreitol, 1 mmol/L phenylmethyl sulfonyl fluoride, and 0.1 mg/mL BSA]. The reactions were resolved on SDS-PAGE and analyzed by Western blot analysis.

SHMT2-specific enzymatic activity assay

SHMT2 activity assay contains two continuous reactions: SHMT2 catalyzes THF and serine to 5, 10-CH_2-THF, and then MTHFD2 catalyzes the 5,10-CH_2-THF to 10-CH_2-THF accompanied with NAD(P)H production, which can be measured (37). Different states of SHMT2 proteins and same quantity GST-MTHFD2 proteins were subjected into activity assay buffer, and increase in absorbance at 350 nm was measured every minute for 30 minutes at 37°C. THF, serine, NAD^+, and $NADP^+$ are substrates and PLP or $MgCl_2$ are activators of SHMT2 or MTHFD2, respectively. Reaction mixture consists of 50 mmol/L Tris-HCl (pH 8.0), 100 mmol/L NaCl, 5 mmol/L $NADP^+$, 2 mmol/L NAD^+, 2 mmol/L THF, 0.5 mmol/L serine, 0.5 mmol/L PLP, 5 mmol/L $MgCl_2$, 1 mg/mL BSA, and 10% glycerol. Data of enzyme activities were from at least triplicate wells.

NADPH/$NADP^+$ ratio assay

Cells were treated in the presence or absence of serine/glycine for 36 hours before experiments. Cells (1×10^6) were harvested and lysed by freeze/thawing. Cell lysates were deproteinized by filtering through 10 kDa cut-off spin filter (Amicon Ultra 10 K device). NADPH/$NADP^+$ ratio was measured by following the manufacturer's instructions of NADP/NADPH Quantification Kit (MAK038, Sigma-Aldrich)

GSH/GSSG ratio assay

Cells were treated in the presence or absence of serine/glycine for 24 hours before experiments. Cells were harvested and GSH/GSSG ratio was measured by following the manufacturer's instructions of GSH/GSSG Assay Kit (S0053, Beyotime).

Cellular reactive oxygen species assay

Cells were treated in the presence or absence of serine/glycine for 36 hours before experiments. Cells (1×10^4) were reseeded into 96-well plates overnight. Reactive oxygen species (ROS) level was measured by Fluorometric Intracellular ROS Kit (MAK145, Sigma-Aldrich) after adding menadione the next day.

Cell proliferation and colony formation

For all cell proliferation experiments, cells were initially seeded into 6-well plates at 5.0×10^4 cells. For serine/glycine starvation treatment, cell medium was changed 16 hours after seeding; from this time point, cells were trypsinized and counted every day (Countstar IC1000, Inno-Alliance Biotech). For the colony formation assay, 1.0×10^4 cells were seeded in 6-cm dishes and kept under different medium or different regent(s) treatment for 7 days. Cells were fixed by 4% paraformaldehyde and stained with 0.2% crystal violet solution and photographed using a digital scanner. Relative growth was quantified by extracting crystal violet from the stained cells using 30% of acetic acid. Collected acetic acid was measured in absorbance at 570 nm.

Metabolite extraction and UPLC-MS/MS

For glycine and serine analysis, cells in different stages were washed and digested. A total of 500 μL 80% methanol extraction solvent (methanol/water 4:1 v/v) and 200 ng/mL glibenclamide (internal standard) was added, and the samples were allowed to equilibrate on ice for 2 minutes. Cells were sonicated and centrifuged at 14,000 × *g* for 10 minutes. Supernatant was deproteinized by filtering through a 10 kDa cut-off spin filter. Metabolites were dried under vacuum and resuspended in 50 μL water, and 5 μL sample was used for analysis.

The Ultimate 3000 UHPLC system was coupled to Q-Exactive MS (Thermo Fisher Scientific) for metabolite separation and detection (38). Metabolites were quantified using peak area, and Student *t* test was used to analyze the differences between groups.

Wound healing assay

Different states of cells were seeded into 6-well cell culture plate and cells overgrew the dish around 24 hours. Then, cells were wounded with a sterile yellow plastic tip. Cell migration was observed and photographed by microscopy (Eclipse TS100, Nicon) several hours later.

Xenograft experiment

HCT116-rescued SHMT2 WT or SHMT2 K280E stable cells were trypsinized and counted. Then, 1×10^7 cells resuspended in PBS were mixed with MaxGel ECM (E0282, Sigma-Aldrich) at 1:10 (v/v) and injected into right anterior armpit of 4- to 6-week-old male BALB/c nude mice (Charles River Laboratories). Four weeks after injection, mice were sacrificed, and tumors were dissected and photographed by camera. The weight and volume of tumors were measured. The volume calculated formula: $V = \pi \times \text{length} \times \text{width}^2/6$. All studies related to animals were approved by the Peking University Health Science Center Institutional Animal Care and Use Committee.

Statistical analyses

Statistical analyses were performed with a two-tailed unpaired Student *t* test by SPSS 20. All data represented in the figures with SEM (mean ± SD). A difference was considered statistically significant at a value of $P < 0.05$. * denotes $P < 0.05$, ** denotes $P < 0.01$, and *** denotes $P < 0.001$, which were considered statistically significant.

Results

SHMT2 identified from SIRT5 interaction network

SIRT5 is defined as the metabolism regulator for its multiple protein deacylation function. To explore SIRT5 accurate functions in cellular metabolism, we generated a C-terminal Flag-tagged SIRT5 construct (Fig. 1A) and overexpressed in HEK293T cells. Mitochondria was isolated from cells (36) and extracted proteins were immunoprecipitated by M2 beads (Fig. 1B). The interacting proteins coprecipitated with the SIRT5-FLAG were eluted and visualized by Coomassie blue staining (Fig. 1C, repeated in four independent experiments). All proteins were identified by mass spectrometry. We found that SIRT5 interacts with multiple proteins that belong to several cellular metabolism pathways (Fig. 1D). We randomly chose several proteins (peptides identified are shown in Supplementary Fig. S1A) for SIRT5 coimmunoprecipitation and confirmed the interactions (Supplementary Fig. S1B–S1E). Of note, a total of 16 peptides were identified for SHMT2 protein from 53 kDa band (Fig. 1C), and the peptides in this analysis covered 34.2% of SHMT2 (Supplementary Fig. S1A), indicating the strong interaction of these two proteins. We also performed a SIRT5 desuccinylation assay with these proteins, and coexpression of the same set of proteins with SIRT5 showed reduced succinylation levels of several proteins (Supplementary Fig. S1F), confirming that our purified SIRT5-interacted proteins are indeed in SIRT5-related succinylome.

To further confirm the interaction between these proteins, SIRT5 and SHMT2 constructs were transiently transfected into the HEK293T cells. SHMT2 can clearly be coimmunoprecipitated by the SIRT5-FLAG (Supplementary Fig. S1G), and SIRT5 can be coimmunoprecipitated by the SHMT2-FLAG (Supplementary Fig. S1H). To examine the interaction of endogenous SIRT5 and SHMT2, U2OS whole-cell lysates were incubated with control IgG, anti-SHMT2, or anti-SIRT5 antibodies, and immunoprecipitates were detected by anti-SIRT5 and anti-SHMT2 antibodies. Endogenous SHMT2 was coprecipitated with endogenous SIRT5 from U2OS cell lysates, but not from control IgG (Fig. 1E). Conversely, endogenous SIRT5 was also coprecipitated with endogenous SHMT2 (Fig. 1F). We also performed the GST-pulldown assay and confirmed that SIRT5 can interact with SHMT2 *in vitro* (Fig. 1G).

As SIRT5 contains multiple enzymatic activities, we first determined which dominant PTM that SHMT2 is regulated by SIRT5. Cells transfected with Flag-SHMT2 were treated with nicotinamide, and Flag-SHMT2 proteins were precipitated and Western blotted with different PTM antibodies. SHMT2 was slightly glutarylated and strongly acetylated and succinylated (Supplementary Fig. S1I). Instead of nicotinamide treatment, the SIRT5-overexpressing cells underwent the same set of experiments. SHMT2 was slightly deglutarylated and strongly desuccinylated (Fig. 1H; Supplementary Fig. S1J). However, SHMT2 acetylation levels were increased in SIRT5-overexpressing cells (Supplementary Fig. S1J) and slightly decreased in SIRT3-overexpressing cells (Supplementary Fig. S1K). Together, these data indicate the major PTM of SHMT2 is controlled by SIRT5 is succinylation.

SIRT5 is irreplaceable for cancer cells in response to serine/glycine deprivation

Using the CRISPR/Cas9 technique (39), we knocked out SIRT5 in U2OS cells. Among the 21 KO clones obtained, we chose two of them for the experiments (SIRT5 KOΔa and SIRT5 KOΔb). SIRT5 was clearly knocked out in both cell lines (Supplementary Fig. S2A and S2B). We also examined the profile of protein expression and PTM for both cell lines. The protein expression was not changed in both cell lines (Supplementary Fig. S2C, Ponceau S stain). Surprisingly, the total protein acetylation and glutarylation levels were slightly reduced in both KO cell lines; however, the total succinylation levels were significantly increased (Supplementary Fig. S2C), indicating that SIRT5 prefers to regulate cancer cell cellular succinylome.

We examined the cellular response to serine/glycine starvation in these cell lines. Serine/glycine–starved SIRT5 WT and KO cells were affected to different degrees: SIRT5 KO cells showed a much lower $NADPH/NADP^+$ ratio (Fig. 2A; Supplementary Fig. S2D), a lower GSH/GSSH ratio (Fig. 2B), higher cellular ROS level (Fig. 2C; Supplementary Fig. S2E), and lower cell growth rate (Fig. 2D; Supplementary Fig. S2F) under serine/glycine starvation than WT cells. In detail, serine/glycine–starved versus supplied SIRT5 WT cells showed 56.1% decreasing $NADPH/NADP^+$ ratio in comparison with over 80% decreasing of SIRT5 KO cells in Fig. 2A, and SIRT5 WT cells showed <5% decreasing GSH/GSSG ratio in comparison with 35% decreasing of SIRT5 KO cells under serine/glycine deprivation in Fig. 2B. Consistently, in Fig. 2D, serine/glycine–starved versus supplied SIRT5 WT cells showed 33.5% decreasing of cell growth rate in comparison with 57.9% decreasing of SIRT5 KO cells. Furthermore, we found that the function of SIRT5 on regulating nonessential amino acid metabolism was not universal. Although asparagine can promote tumor cell growth (40) and aspartate is the material for *de novo* asparagine synthesis, SIRT5 KO cells showed the same pattern on metabolic index change and cell growth rate change as SIRT5 WT cells under aspartate/asparagine starvation (Supplementary Fig. S2G–S2J), indicating the specificity of the involvement of SIRT5 on serine/glycine metabolism. The metabolic flux from

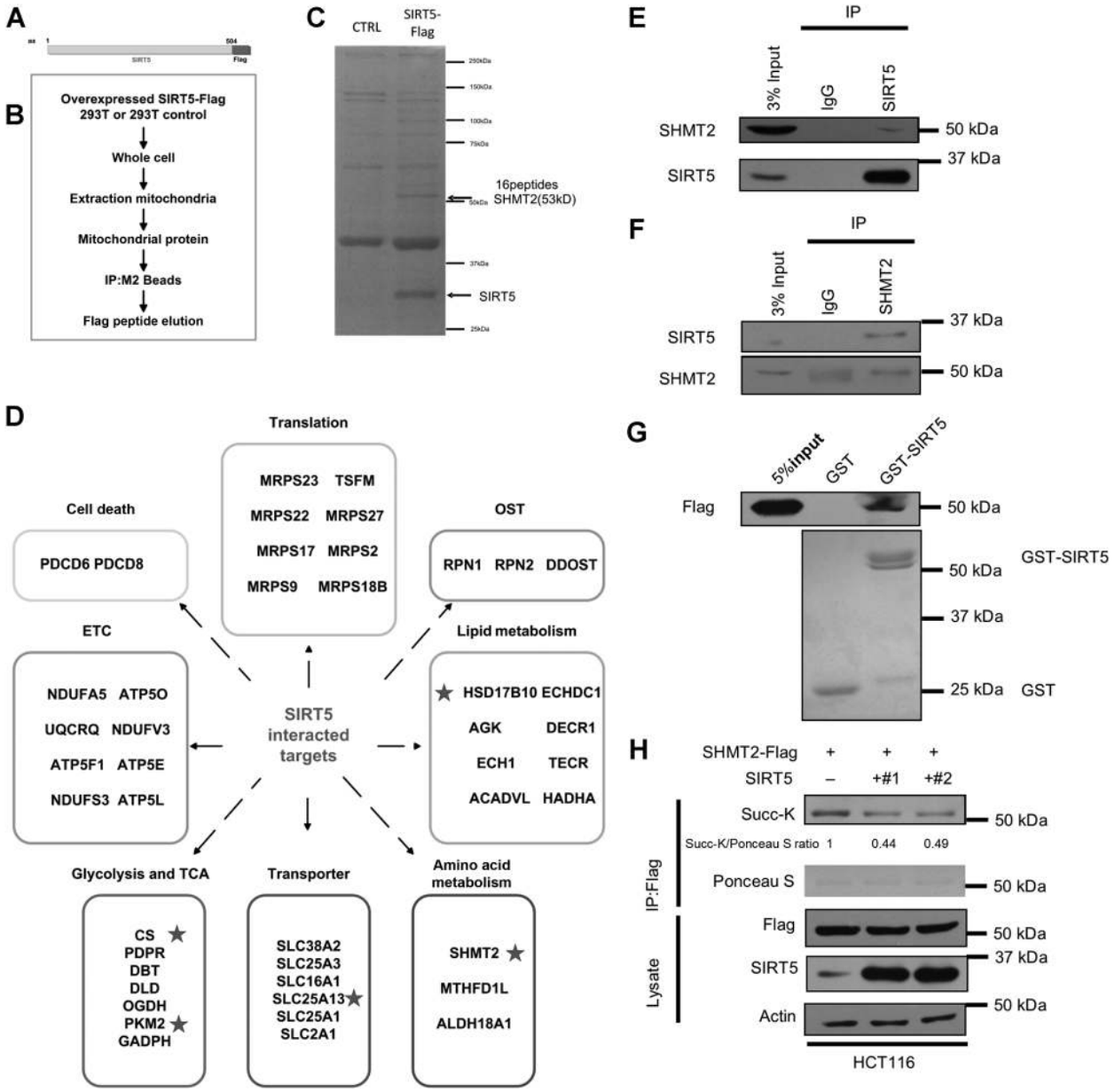

Figure 1.

SHMT2 identified from SIRT5 interaction network. **A** and **B,** Schematic representation of C-terminal Flag-tagged SIRT5 plasmid (**A**) and strategy of SIRT5-interacted protein identification (**B**). **C,** Immunopurification and mass spectrometry analysis of SIRT5-associated proteins. The Flag peptide elution was subjected to SDS-PAGE and Coomassie blue staining. The protein bands were cut and analyzed by mass spectrometry. **D,** SIRT5-associated protein network. SIRT5-interacted proteins were divided into several cellular metabolism pathways. **E** and **F,** SIRT5 interacts with SHMT2 *in vivo*. Whole-cell lysates were immunoprecipitated with control IgG, anti-SIRT5, or anti-SHMT2 antibodies, and precipitated proteins were detected by anti-SHMT2 or anti-SIRT5 antibodies, respectively. **G,** SIRT5 interacts with SHMT2 *in vitro*. GST pull-down assay with GST-fused SIRT5 and Flag-tagged SHMT2 proteins. **H,** SIRT5 regulates succinylation of SHMT2. HCT116 cells were cotransfected with Flag-tagged SHMT2 and SIRT5 plasmids. Precipitated proteins were analyzed by Western blot analysis. Relative succinylation level was quantified.

serine to glycine had 15% reduction in SIRT5 KO cells under serine/glycine starvation (Fig. 2E). In addition, SIRT5 KO cells showed decreased ability for clonogenic growth (Fig. 2F). Formate is the product of mitochondrial folate metabolism and fuels cytosolic one-carbon metabolism for purine synthesis (Supplementary Fig. S2K). Formate supplementation can restore the serine deficiency–induced cell proliferation inhibition (9). Replenishing formate to SIRT5 WT or SIRT5 KO cells, which were under serine/glycine starvation, the results showed that WT cells can recover their clonogenic growth, but the KO cells showed less ability of the recovery (Fig. 2G). Consistent with this, either GSH or NAC supplementation in the serine/glycine–starved medium

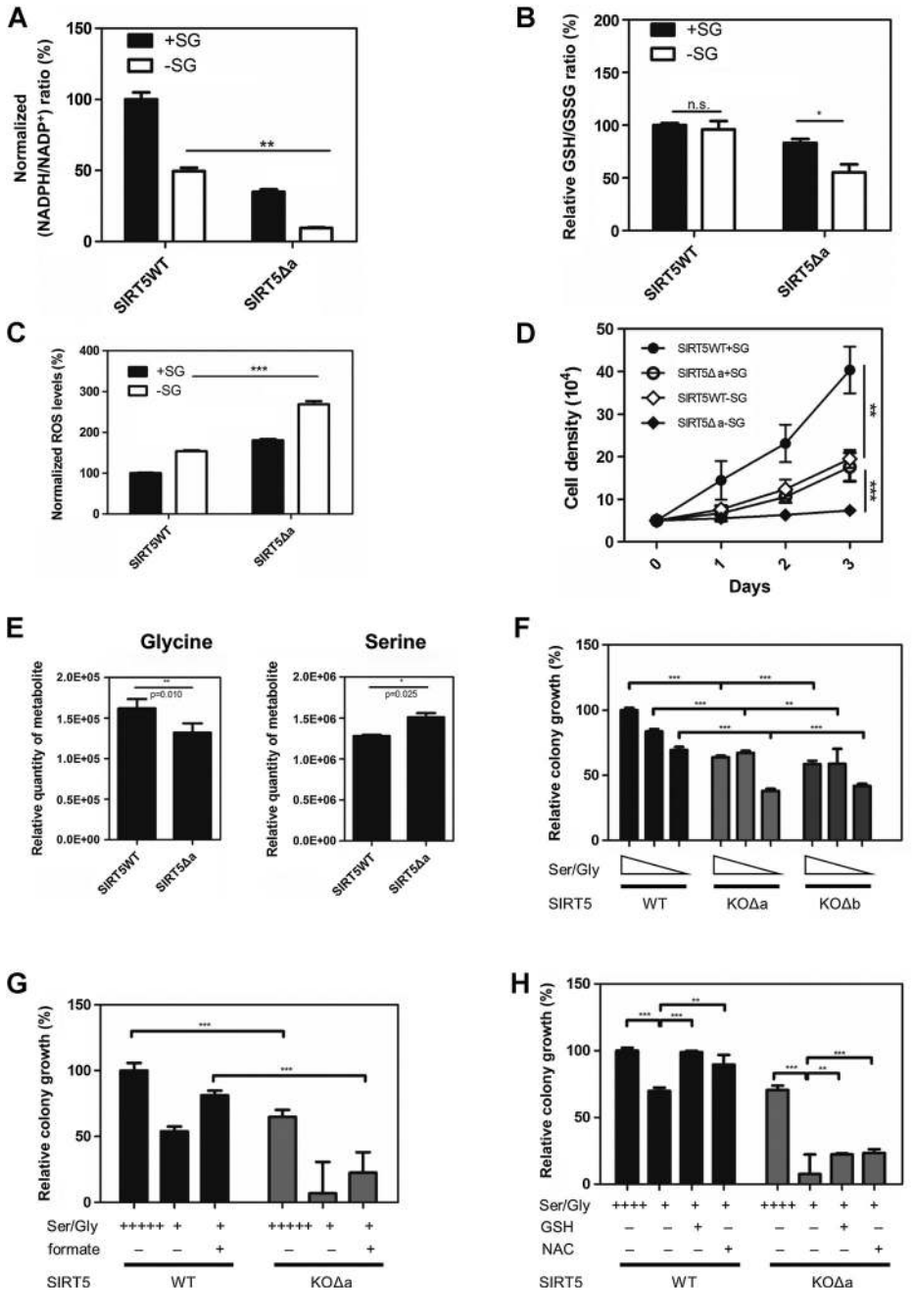

Figure 2.

SIRT5 is irreplaceable for cancer cells in response to serine/glycine deprivation. **A,** SIRT5 KO decreases cellular NADPH/$NADP^+$ ratio under serine/glycine starvation. U2OS SIRT5 WT cells or SIRT5 KO Δa cells were treated in the presence (+SG) or absence (−SG) of serine/glycine for 36 hours. Cells' cellular NADPH/$NADP^+$ ratio was measured. **B,** SIRT5 KO decreases cellular GSH/GSSG ratio under serine/glycine starvation. U2OS SIRT5 WT cells or SIRT5 KO Δa cells were treated in the presence or absence of serine/glycine for 36 hours. GSH/GSSG ratio in cells was measured. **C,** SIRT5 KO increases cellular ROS under serine/glycine starvation. U2OS SIRT5 WT cells or SIRT5 KO Δa cells were treated in the presence or absence of serine/glycine for 36 hours. Cells were reseeded into 96-well plates, and ROS level was measured by adding 10 μmol/L menadione. **D,** SIRT5 KO restrains cell proliferation. U2OS SIRT5 WT cells or SIRT5 KO Δa cells were seeded into 6-well plates at the same number with or without serine/glycine. Cell numbers were counted every day. **E,** Reducing serine catabolism flux in SIRT5 KO cells. U2OS SIRT5 WT cells or SIRT5 KOΔa cells were serine/glycine starved for 36 hours before harvest. Metabolites from cells were analyzed by UPLC–MS/MS. Relative quantity of metabolites are shown (*y* axis = peak area). **F,** SIRT5 KO inhibits cell clonogenic growth. U2OS SIRT5 WT cells or SIRT5 KO Δa/Δb cells were seeded into 6-cm dishes at the same number in the presence of serine/glycine at descending concentration. Clonogenic growth was determined. **G,** Formate restores cell clonogenic growth of SIRT5 WT rather than KO cells. U2OS SIRT5 WT or SIRT5 KO Δa cells cultured in serine/glycine–deprived medium were resupplied with 1 mmol/L formate. Clonogenic growth was determined. **H,** GSH or NAC restores cell clonogenic growth of SIRT5 WT rather than KO cells. U2OS SIRT5 WT or SIRT5 KO Δa cells cultured in serine/glycine–deprived medium were resupplied with 250 μmol/L GSH or 250 μmol/L NAC. Clonogenic growth was determined. Error bars, ±SD ($n \geq 3$). n.s., nonsignificant, $P \geq 0.05$; *, $P < 0.05$; **, $P < 0.01$; ***, $P < 0.001$ for the indicated comparison.

rescued growth of SIRT5 WT cells, but the KO cells showed less ability of the recovery (Fig. 2H), indicating that SIRT5 is an important regulator among the one-carbon metabolism for cell proliferation. We also examined the key protein expression levels in response to serine/glycine starvation. SIRT5 KO cells showed reduced levels of voltage-dependent anion-selective channel protein (VDAC). However, SHMT2 and PKM2 levels remained the same in response to serine/glycine starvation (Supplementary Fig. S2L), suggesting that these proteins may regulate their enzymatic activities through PTM rather than changing protein expression levels.

SIRT5 desuccinylates SHMT2 *in vivo* and *in vitro*

With different amounts of succinyl-CoA, *in vitro* assay showed that SHMT2 succinylation levels were dose dependent (Fig. 3A). The *in vitro* succinylation of protein is a nonenzymatic reaction (41) and succinyl-CoA is a reactive agent for protein modification (42). In addition, SHMT2 succinylation levels were increased in cells treated with nicotinamide but not with sodium butyrate, suggesting that SHMT2 succinylation levels were regulated by class III not the class I or II HDACs (Fig. 3B). SIRT5 desuccinylated SHMT2 in cells in a dose-dependent manner (Fig. 3C). We also examined the SHMT2 succinylation with all three mitochondrial sirtuins. Only SIRT5 showed strongest desuccinylation effects on SHMT2 (Fig. 3D). However, SIRT5 enzymatically defective mutant SIRT5-H158Y failed to desuccinylate SHMT2 (Fig. 3E). Consistently, a SIRT5 N-terminal deletion mutant SIRT5Δ50, which cannot enter the mitochondria, failed to desuccinylate SHMT2 (Fig. 3F). Overexpression of SHMT2 in SIRT5-deficient cells strongly increased its succinylation levels (Fig. 3G; Supplementary Fig. S3A). Endogenous SHMT2 succinylation levels were also increased in SIRT5-deficient cells (Fig. 3H). Notably, only WT SIRT5, not SIRT5-H158Y or SIRT3, can desuccinylate SHMT2 *in vitro* (Fig. 3I). All these results indicate that SIRT5 desuccinylates SHMT2 both *in vivo* and *in vitro*.

SIRT5 upregulates SHMT2 enzymatic activity under metabolic stress

To investigate the physiologic functions of the SIRT5-SHMT2 regulation, we first examined its effect on SHMT2 enzymatic activities. Cells treated with nicotinamide, which increased SHMT2 succinylation levels, reduced the SHMT2 activity (Fig. 4A). Overexpression of SIRT5 in cells increased SHMT2 activity (Fig. 4B). In addition, SIRT5 KO cells, which showed increased SHMT2 succinylation levels, reduced the SHMT2 activity (Fig. 4C; Supplementary Fig. S4A). *In vitro* succinylated recombination SHMT2 showed decreased enzymatic activity (Fig. 4D). These data indicate that SHMT2 enzymatic activity is tightly associated with its succinylation levels, which is regulated by SIRT5.

To investigate SIRT5-SHMT2 regulation in response to metabolic stress, we first examined the SHMT2 succinylation levels under serine/glycine starvation. The succinylation levels of SHMT2 were reduced in response to serine/glycine deprivation in HCT116 cells both with overexpressed SHMT2 (Fig. 4E) or endogenous SHMT2 (Fig. 4F). Coimmunoprecipitation assay was also performed in cells with or without serine/glycine, and we can clearly detect the increased interaction between SIRT5 and SHMT2 proteins under serine/glycine deprivation (Fig. 4G). Accompanied with reduced succinylation levels of SHMT2, the enzymatic activities were increased significantly as expected (Fig. 4H). Furthermore, we treated HCT116 cells with DMHG, which can enhance protein succinylation levels through cellular succinate accumulation (33), and found that the total protein succinylation levels and SHMT2 succinylation levels were both slightly increased (Supplementary Fig. S4B and S4C). However, the slightly increased succinylation levels of SHMT2 under DMHG treatment were strongly reversed under serine/glycine deprivation (Supplementary Fig. S4B and S4C), suggesting that the succinylation levels of SHMT2 were strongly regulated by serine/glycine starvation despite the cellular hypersuccinylated state. The transcriptional (Supplementary Fig. S4D) or translational (Supplementary Fig. S4E) regulation on SIRT5 was changed slightly when cells were serine/glycine starved, suggesting undiscovered mechanism on SIRT5 upstream regulation. As the materials for *de novo* serine synthesis, glucose is pivotal for cancer cell metabolism. Not surprisingly, HCT116 cells under glucose starvation also showed reduced succinylation levels of SHMT2 in response to glucose deprivation (Supplementary Fig. S4F). All these results demonstrated that the desuccinylation of SHMT2 by SIRT5 increased its enzymatic activity in response to metabolic stress.

K280 is the major succinylation site of SHMT2

To identify the succinylation sites on SHMT2, we purified succinylated SHMT2 protein from cells and examined its succinylation sites through mass spectrometry. Seven lysine residues (K103, K280, K302, K356, K464, K469, and K474) were identified as candidate sites. We mutated all these lysines to arginines (R; mimicking the desuccinylated state) or glutamic acids (E; mimicking the negatively charged succinyllysine modification) and examined their succinylation levels and enzymatic activities, respectively. As shown in Fig. 5A and B, both K280R and K280E showed lower succinylation levels and enzymatic activities significantly, indicating that K280 is the key succinylation site for SHMT2 enzymatic activity and functions. Although the other SHMT2 mutants also showed change in succinylation levels, the enzymatic activities of SHMT2 proteins were not significantly changed, suggesting that these sites were the nonessential succinylated sites for SHMT2 activity. Crystal structure of SHMT2 proteins showed that K280 bounded to succinyl group prevented PLP binding (Fig. 5C), and SHMT2 K280E mutant lowers its binding ability to PLP consequently by mimicking the negatively charged succinyllysine modification (Supplementary Fig. S5A). Moreover, K280 is a highly conserved site: It has remained the same from yeast to humans (Supplementary Fig. S5B). We also found that SHMT2 K280R was a succinylation regulation–resistant mutant. K280R showed lower enzymatic activity whether the cells were under DHMG or serine/glycine–starved treatment (Supplementary Fig. S5C). The abovementioned results demonstrated that succinylation can regulate SHMT2 enzymatic activity at K280.

As most of SHMT2 proteins form homodimers in cells without enzymatic activity, they must form tetramers to become active forms (2). Therefore, we further investigated whether K280E, which lowered the enzymatic activity of SHMT2 (Fig. 5B), affects its tetramer formation. Indeed, tetramers formed less in K280E than WT both in whole-cell lysates and immunoprecipitation products (Fig. 5D). This result indicates that K280 is important for its tetramer formation and enzymatic activity. In addition, compared with WT SHMT2, the succinylation levels of K280E mutant were unchanged in response to serine/glycine starvation,

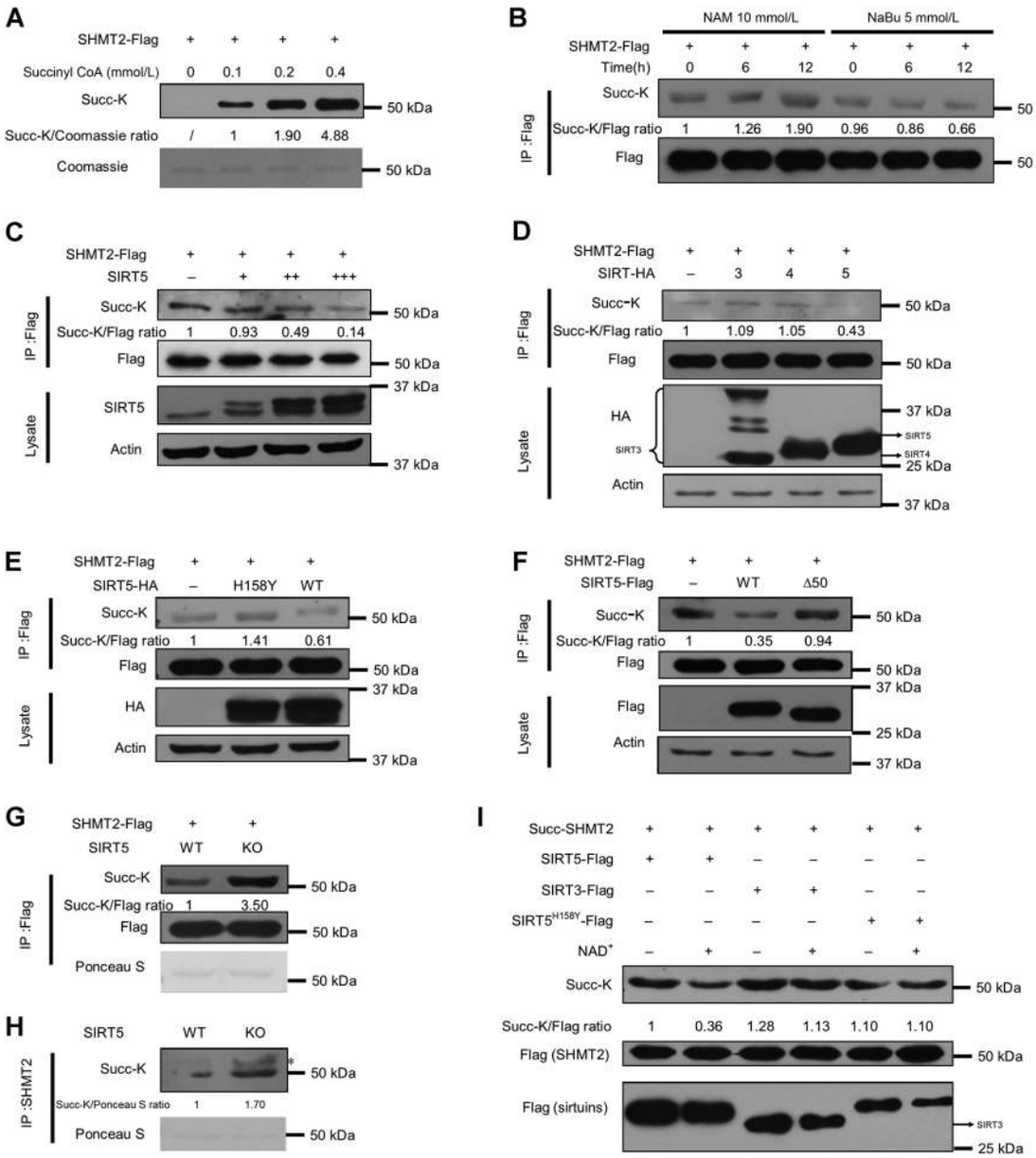

Figure 3.

SIRT5 desuccinylates SHMT2 *in vivo* and *in vitro*. **A,** *In vitro* SHMT2 succinylation assay. SHMT2 proteins were incubated with different concentrations of succinyl-CoA as indicated. Protein succinylation level was analyzed, and loading proteins were stained by Coomassie blue. Relative succinylation level was quantified. **B,** SHMT2 succinylation is not controlled by HDAC class I/II. Succinylation of ectopically expressed SHMT2 proteins from HEK293T cells was analyzed after different treating time of nicotinamide or sodium butyrate (NaBu). Relative succinylation level was quantified. **C,** SIRT5 desuccinylates SHMT2 in a dose-dependent manner. HEK293T cells were cotransfected with plasmids that express Flag-tagged SHMT2 and increasing amounts of SIRT5. Relative succinylation level was quantified. **D,** SIRT5, instead of other mitochondrial sirtuins, decreases SHMT2 succinylation level. HEK293T cells were cotransfected with Flag-tagged SHMT2 and HA-tagged SIRT3, SIRT4, or SIRT5. Precipitated SHMT2 proteins or ectopically expressed SIRT3, SIRT4, or SIRT5 were determined. Relative succinylation level was quantified. **E,** Overexpression of SIRT5, not SIRT5 enzymatic-defective mutant, decreases SHMT2 succinylation level. HEK293T cells were cotransfected with plasmids that express Flag-tagged SHMT2 and HA-tagged SIRT5 or SIRT5-H158Y. Succinylation of SHMT2 proteins was determined. Relative succinylation level was quantified. **F,** SIRT5 mainly desuccinylates SHMT2 in mitochondria. Flag-tagged SHMT2 and Flag-tagged SIRT5 or mitochondrial transit peptide defective SIRT5Δ50 were cotransfected into HEK293T cells. Succinylation of precipitated SHMT2 was determined. Relative succinylation level was quantified. **G,** SIRT5 KO increases overexpressed SHMT2 succinylation level. U2OS SIRT5 WT and SIRT5 KO Δa cells were transfected with Flag-tagged SHMT2. Immunoprecipitated SHMT2 was analyzed with anti–pan-succinyllysine. Relative succinylation level was quantified. **H,** SIRT5 KO increases endogenous SHMT2 succinylation level. U2OS SIRT5 WT cells or SIRT5 KO Δa cell lysates were immunoprecipitated with anti-SHMT2 antibody. Succinylation levels of endogenous SHMT2 proteins were detected by anti–pan-succinyllysine or Ponceau S staining. Relative succinylation level was quantified. **I,** *In vitro* SHMT2 desuccinylation assay. Succinylated Flag-tagged SHMT2 proteins were incubated with purified SIRT3, SIRT5, or SIRT5-H158Y proteins, respectively, in the presence or absence of NAD^+ for 1 hour at 30°C. Proteins were analyzed by Western blot analysis. Relative succinylation level was quantified.

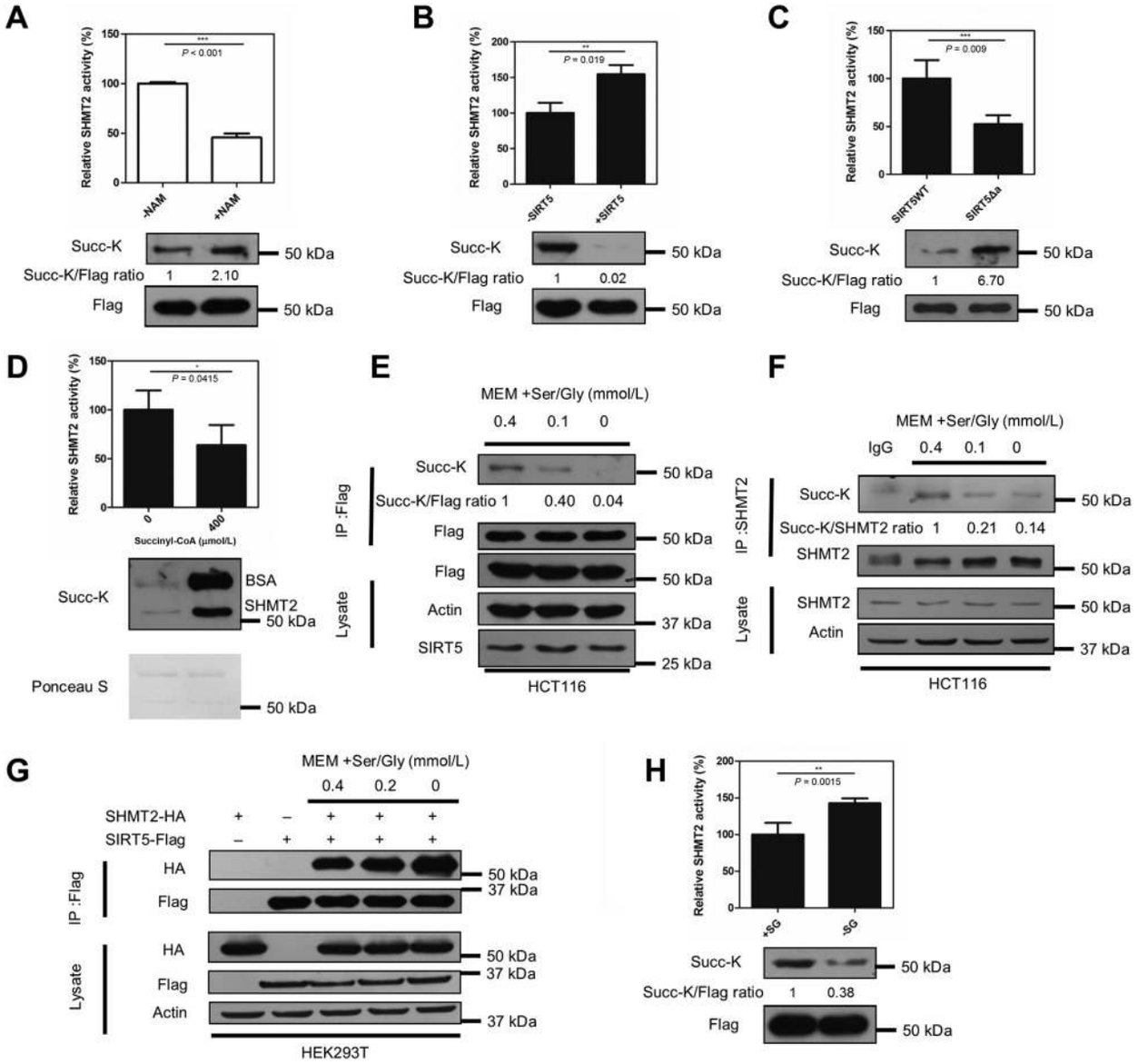

Figure 4.

SIRT5 upregulates SHMT2 enzymatic activity under metabolic stress. **A,** Sirtuins inhibitor nicotinamide represses SHMT2 activity. HEK293T cells were transfected with Flag-tagged SHMT2 and treated with or without nicotinamide for 6 hours. Purified SHMT2 activity was detected by specific enzymatic assay. Error bars, ±SD ($n = 4$). **B,** SIRT5 activates SHMT2. HEK293T cells were cotransfected with Flag-tagged SHMT2 with or without SIRT5. SHMT2 proteins were purified and detected by specific enzymatic activity assay. Error bars, ±SD ($n = 3$). **C,** SIRT5 KO decreases SHMT2 activity. U2OS SIRT5 WT or SIRT5 KO Δa cells were transfected with Flag-tagged SHMT2. Purified SHMT2 activity was detected by specific enzymatic assay. Error bars, ±SD ($n = 3$). **D,** *In vitro* succinylation of SHMT2 decreases its activity. SHMT2 proteins were purified and incubated with or without 400 μmol/L succinyl-CoA for 15 minutes at 30°C before specific enzymatic assay. Error bars, ±SD ($n = 3$). **E,** SIRT5 desuccinylates overexpressed SHMT2 under serine/glycine starvation. HCT116 cells were transfected with Flag-tagged SHMT2 and treated with different serine/glycine concentration medium as indicated for 36 hours. Precipitated SHMT2 proteins were analyzed with anti–pan-succinyllysine antibody. Relative succinylation level was quantified. **F,** SIRT5 desuccinylates endogenous SHMT2 under serine/glycine starvation. HCT116 cells were treated with different serine/glycine concentration medium as indicated for 36 hours. Precipitated SHMT2 proteins were analyzed with anti–pan-succinyllysine antibody. Relative succinylation level was quantified. **G,** SIRT5 interacts with SHMT2 under serine/glycine starvation. HEK293T cells were cotransfected with Flag-tagged SIRT5 and HA-tagged SHMT2 and treated with different serine/glycine concentrations as indicated for 36 hours. Cell lysates were immunoprecipitated and detected by Flag and HA antibodies. **H,** Activation of SHMT2 in response to serine/glycine starvation. U2OS cells were transfected with Flag-tagged SHMT2 and treated in the presence or absence of serine/glycine for 36 hours. SHMT2 proteins were purified for specific enzymatic assay. Error bars, ±SD ($n = 3$).

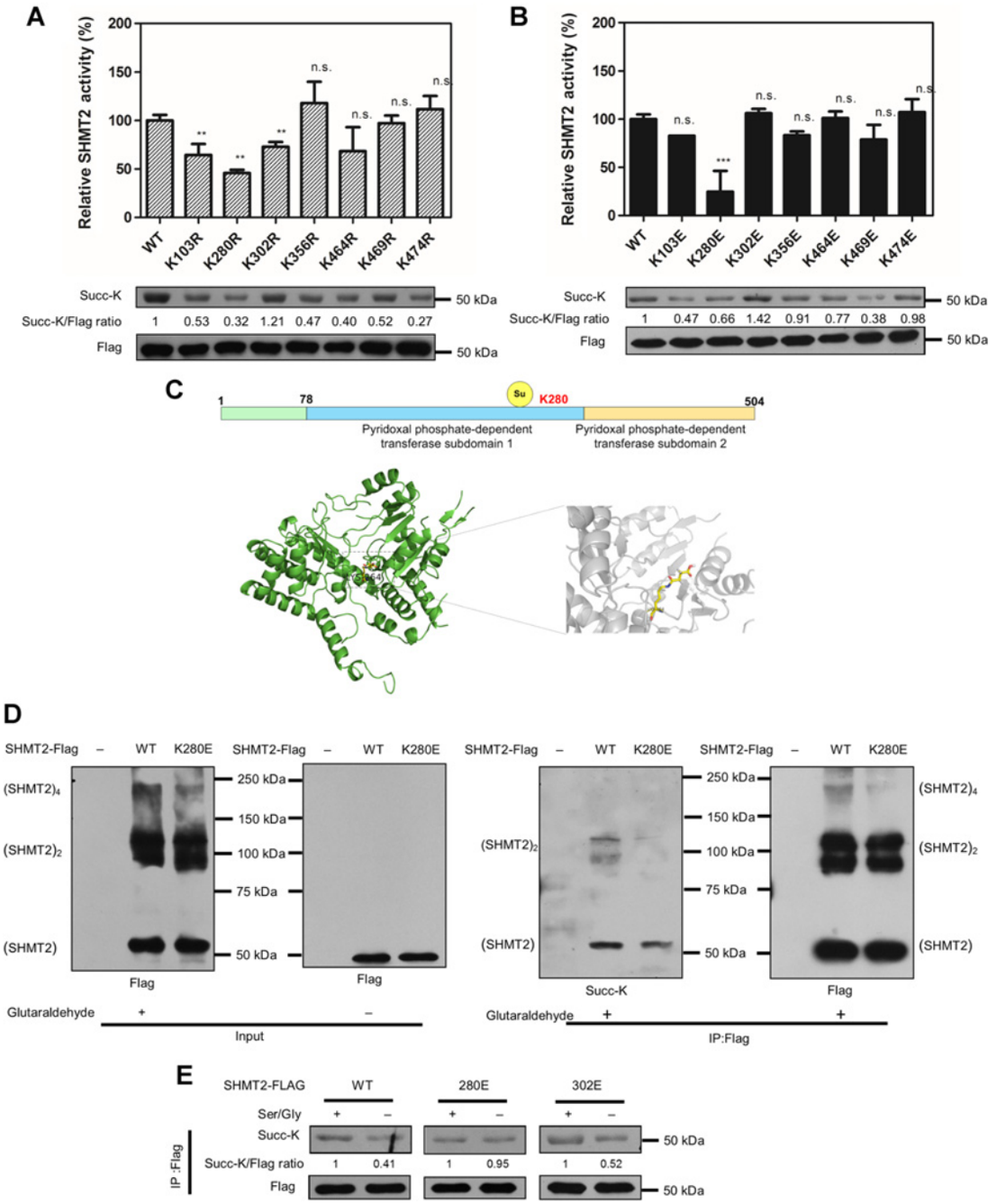

Figure 5.

K280 is the major succinylation site of SHMT2. **A,** Mapping the major lysine PTM sites of SHMT2. SHMT2 WT and seven indicated K to R mutants constructs were transfected into HEK293T cells, and enzymatic activity of purified SHMT2 proteins was detected by specific enzymatic assay. Succinylation levels of purified SHMT2 proteins were detected. **B,** Mapping the major succinylation sites of SHMT2. SHMT2 WT and seven indicated K to E mutant constructs were transfected into HEK293T cells, and activity of purified SHMT2 proteins was detected by specific enzymatic assay. Succinylation levels of purified SHMT2 proteins were detected. Error bars, ±SD ($n = 3$). n.s., nonsignificant, $P \geq 0.05$; **, $P < 0.01$; ***, $P < 0.001$ for the indicated comparison. **C,** Top, schematic representation of SHMT2 with K280 identified in proteomics; bottom, crystal structure of SHMT2 proteins (2.04 Å) with K280 (K264 in PDB ID 3OU5) bounded with succinyl group. The SHMT2 homodimer is shown in green chains and succinyl group is shown in stick format. Bottom right view is enlarged to show that succinyl group binds to K280 of SHMT2. **D,** K280E mutation disturbs SHMT2 tetramerization. Cell lysates of HEK293T cells expressing Flag-tagged WT SHMT2 or K280E mutant were treated with or without 0.025% glutaraldehyde and analyzed by Western blot analysis with anti-Flag antibody. Succinylation of precipitated SHMT2 proteins was analyzed. Tetramer, dimer, and monomer of SHMT2 are indicated. **E,** Succinylation of SHMT2 K280E is not changed in response to serine/glycine starvation. HEK293T cells were transfected with Flag-tagged WT SHMT2 or indicated K to E mutants separately and treated in the presence or absence of serine/glycine for 36 hours. Precipitated SHMT2 proteins were determined. Relative succinylation level was quantified.

indicating that K280 is the major succinylation site of SHMT2 in response to serine/glycine starvation (Fig. 5E).

Succinylation of SHMT2 at K280 restrains cellular redox balance and clonogenic growth

To further examine the function of SHMT2 K280 succinylation, we first generated SHMT2 KO U2OS cells by the CRISPR/Cas9 technique. Several KO cell lines were obtained and confirmed (Supplementary Fig. S6A and S6B). All the SHMT2 KO cells showed a weaker ability for colony formation in comparison with WT cells (Supplementary Fig. S6C). The SHMT2 KO ΔQ clone was chosen for further experiments. Using this clone, we generated three stably reexpressed cell lines: empty vector, Flag-tagged WT, and K280E mutant of SHMT2. Both SHMT2-reconstituted cells had similar SHMT2 expression levels compared with empty vector stably reexpressed U2OS cells (Fig. 6A).

To evaluate the effect of SHMT2 hypersuccinylation on cellular redox homeostasis, cellular NADPH/$NADP^+$ ratios with or without serine/glycine starvation were measured. As expected, SHMT2 KO reduced the NADPH/$NADP^+$ ratio; SHMT2 WT can mitigate this reduction. However, SHMT2 K280E failed to mitigate this reduction (Fig. 6B). Similarly, SHMT2 KO reduced the GSH/GSSG ratio and SHMT2 WT mitigated this reduction but not SHMT2 K280E (Fig. 6C). Consistently, SHMT2 KO cells and SHMT2 K280E also showed higher cellular ROS levels under serine/glycine starvation than SHMT2 WT (Fig. 6D; Supplementary Fig. S6D).

We next examined the cell clonogenic growth that was regulated by SHMT2 hypersuccinylation. SHMT2 KO or SHMT2 K280E was more sensitive to serine/glycine starvation than SHMT2 WT (Fig. 6E). In comparison with SHMT2 WT, addition of formate, GSH, or NAC can make up the SHMT2 K280E lower enzymatic activity induced cell clonogenic growth inhibition (Fig. 6F). Notably, replenished formate can restore cell clonogenic activity of both SHMT2 WT and SHMT2 K280E (Fig. 6G). These results demonstrated that succinylation of SHMT2 at K280 restrains cellular redox balance and cell clonogenic growth.

Succinylation of SHMT2 at K280 impairs tumor cell growth *in vivo* and *in vitro*

We further investigated the effect of SHMT2 K to E mutant influence on tumor cell growth. U2OS SHMT2 K280E cells showed a dramatically decreased cell proliferation rate (Fig. 7A, left). Consistently, SHMT2 WT cells, but not SHMT2 K280E cells, represented faster migration rates in wound healing assay (Fig. 7B). We repeated the physiologic function of hypersuccinylation SHMT2 using the other cell line. SHMT2 knocked down HCT116 cells were stably reexpressed SHMT2 WT or SHMT2 K280E mutant (Supplementary Fig. S7A). HCT116 rescued SHMT2 WT cells showed an increased cell proliferation rate compared with K280E cells (Fig. 7A, right). HCT116-rescued SHMT2 WT cells also showed faster migration rates than K280E cells (Supplementary Fig. S7B), which was consistent with the results from U2OS cells (Fig. 7B). These results demonstrated that succinylation of SHMT2 at K280 impairs cancer cell proliferation.

Compared with the SHMT2 WT–rescued cells, SHMT2 K280E–rescued cells showed increased serine quantity and decreased glycine quantity, indicating significant serine catabolism flux block controlled by SHMT2 K280E (Fig. 7C). K280E represented enzymatic activity deficit phonotype (Fig. 5B), which limited the metabolic reaction from serine to glycine and subsequent one-carbon metabolism, so as to interpret the cell growth limitation by SHMT2 K280E mutant.

To investigate the physiologic significance of K280 hypersuccinylation in tumor growth *in vivo*, we performed xenograft experiments. BALB/c nude mice were subcutaneously injected with HCT116 rescued cell lines. As shown in Fig. 7D, SHMT2 WT xenografts grew at a much faster rate than those dissected from SHMT2 K280E xenografts at the time of harvesting. The tumor from mice injected with SHMT2 K280E cells showed 62.6% and 56.1% in volume and weight decline, respectively, in comparison with those tumors from mice injected with SHMT2 WT cells (Fig. 7E and F). These results demonstrated that hypersuccinylation of SHMT2 at K280 impairs cellular metabolism and inhibits cell proliferation and tumor growth *in vivo* and *in vitro*.

Discussion

As a member of the class III histone deacetylase family, SIRT5 is unique with multiple enzymatic activities, including deacetylase, desuccinylase, deglutarylase, and demalonylase activities. The substrates identified from succinylome, glutarylome, and malonylome are proteins mainly located in the mitochondria, suggesting the important role of SIRT5 in regulating functions of mitochondrial proteins. Recent studies reveal that SIRT5 controls several cellular metabolism pathways (21), including urea cycle, glycolysis, and fatty acid oxidation. However, how SIRT5 functions to influence cellular redox levels still remains unclear. In this study, we found that cells deficit with SIRT5 were more sensitive to serine/glycine starvation. SIRT5 deficiency can induce unrecoverable cell proliferation inhibition and redox homeostasis disorder under serine/glycine starvation. Our findings provide another piece of the puzzle in the holistic picture of one-carbon metabolism (Fig. 7G).

Although serine is a nonessential amino acid for humans, it shows pivotal functions for cancer cells (9). Serine catabolism promotes rapid proliferation in tumors by providing one-carbon units for purines and NADPH production, which could support DNA/RNA synthesis and reduce cellular ROS levels, respectively (12, 14). Cancer cells migrating to new tissues are always confronted with a low glucose and serine environment. Cancer cells can remodel their metabolic pathways to overcome these obstacles and accomplish tumor metastasis. TP53 has been identified for its noncancer-associated functions in response to serine depletion and promotes cell proliferation (18). In our study, we found that SIRT5 KO sensitized cell response to serine/glycine starvation by reducing the NADPH/$NADP^+$ ratio and GSH/GSSG ratio, increasing cellular ROS levels, and decreasing cell proliferation rates in comparison with SIRT5 WT cells (Fig. 2). Thus, SIRT5 plays a pivotal role in regulating serine catabolism.

SHMT2, a protein that acts as the bridge linking serine catabolism and one-carbon metabolism, was identified from SIRT5 mitochondria interaction network and interacted with SIRT5 *in vivo* and *in vitro*, and succinylation of SHMT2 is strongly controlled by SIRT5 consequently. Notably, acetylation of SHMT2 was slightly changed by SIRT3 (Supplementary Fig. S1K), although we did find that SHMT2 appeared in our SIRT3 complex (unpublished data; ref. 43). In our study, we demonstrated that SIRT5 regulation of succinylation levels of SHMT2 is enough to modulate SHMT2 in response to serine/glycine starvation. SIRT3 and SIRT5, which interact with each other, are regarded as the PTM keepers inside mitochondria. Lysine sites among mitochondrial

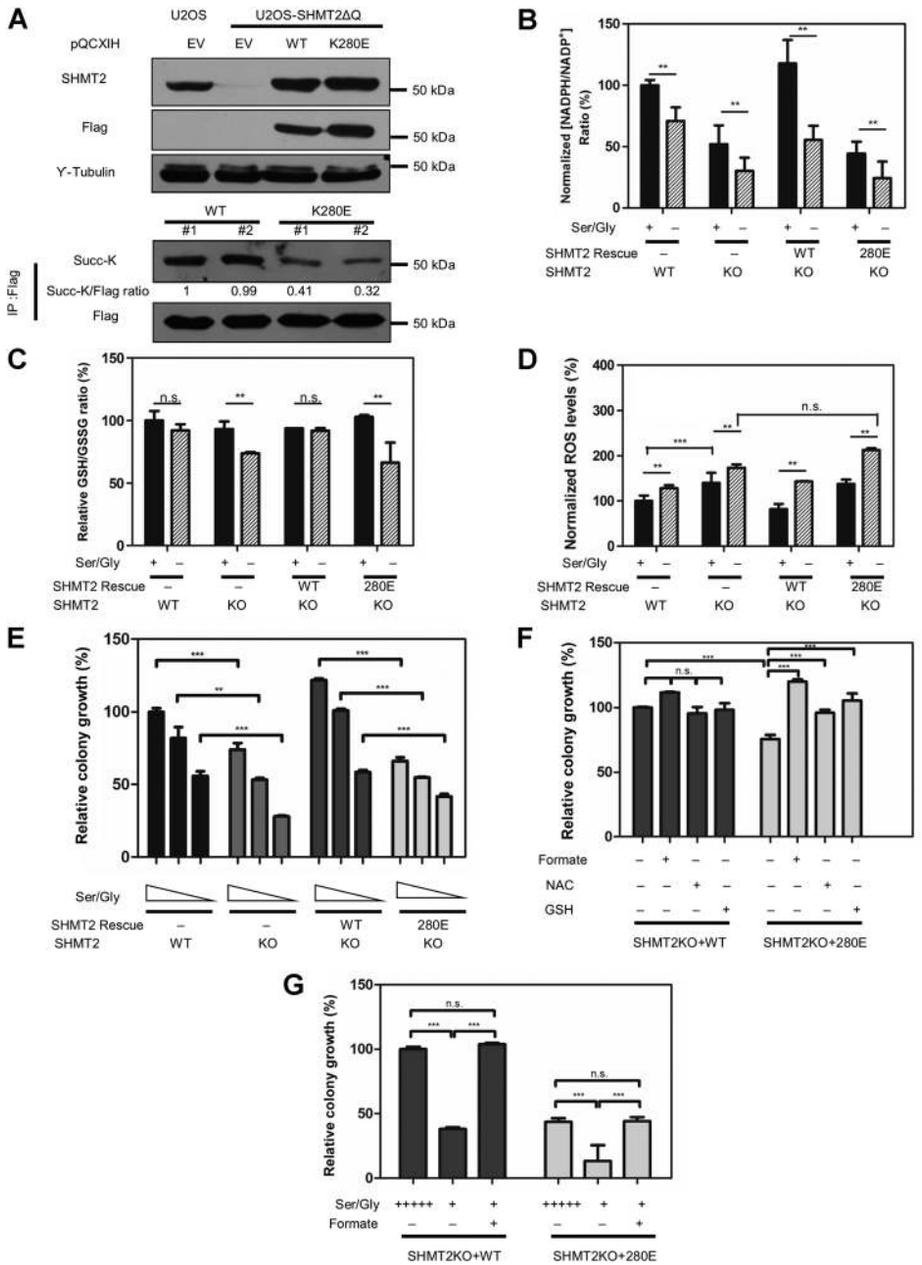

Figure 6.

Succinylation of SHMT2 at K280 restrains cellular redox balance and clonogenic growth. **A,** Identification of U2OS SHMT2 rescued cell lines. SHMT2 was knocked out in U2OS cells and Flag-tagged WT, and 280 K to E mutant of SHMT2 was stably reexpressed in SHMT2 KO cells. Total lysates were prepared from four cell lines and detected by Western blot analysis. WT and K280E SHMT2 proteins were precipitated from $SHMT2^{WT}$ cells or $SHMT2^{K280E}$ cells, respectively. The succinylation levels of SHMT2 proteins were determined. **B,** SHMT2 K280E decreases cellular NADPH/$NADP^+$ ratio under serine/glycine starvation. U2OS WT cells, SHMT2 KO cells, $SHMT2^{WT}$ cells, or $SHMT2^{K280E}$ cells were treated in the presence or absence of serine/glycine for 36 hours. Cells' cellular NADPH/$NADP^+$ ratio was measured. **C,** SHMT2 K280E decreases cellular GSH/GSSG ratio under serine/glycine starvation. U2OS WT cells, SHMT2 KO cells, $SHMT2^{WT}$ cells, or $SHMT2^{K280E}$ cells were treated in the presence or absence of serine/glycine for 36 hours. GSH/GSSG ratio in cells was measured. **D,** SHMT2 K280E increases cellular ROS under serine/glycine starvation. U2OS WT cells, SHMT2 KO cells, $SHMT2^{WT}$ cells, or $SHMT2^{K280E}$ cells were treated in the presence or absence of serine/glycine for 36 hours. Cells were reseeded into 96-well plates at the same number overnight, and ROS level was measured by adding 10 μmol/L menadione. **E,** SHMT2 K280E inhibits cell clonogenic growth. U2OS WT cells, SHMT2 KO cells, $SHMT2^{WT}$ cells, or $SHMT2^{K280E}$ cells were seeded into 6-cm dishes at the same number with descending serine/glycine concentration medium. Clonogenic growth was determined. **F,** Formate, GSH, or NAC restores cell clonogenic growth of $SHMT2^{K280E}$ cells. U2OS $SHMT2^{WT}$ cells or $SHMT2^{K280E}$ cells cultured in normal serine/glycine medium were resupplied with 1 mmol/L formate, 250 μmol/L GSH, or 250 μmol/L NAC. Clonogenic growth was determined. **G,** Formate restores cell clonogenic growth of $SHMT2^{WT}$ cells or $SHMT2^{K280E}$ cells. U2OS $SHMT2^{WT}$ cells or $SHMT2^{K280E}$ cells cultured in serine/glycine–deprived medium were resupplied with 1 mmol/L formate. Clonogenic growth was determined. Error bars, ±SD ($n = 3$). n.s., nonsignificant; **, $P < 0.01$; ***, $P < 0.001$ for the indicated comparison.

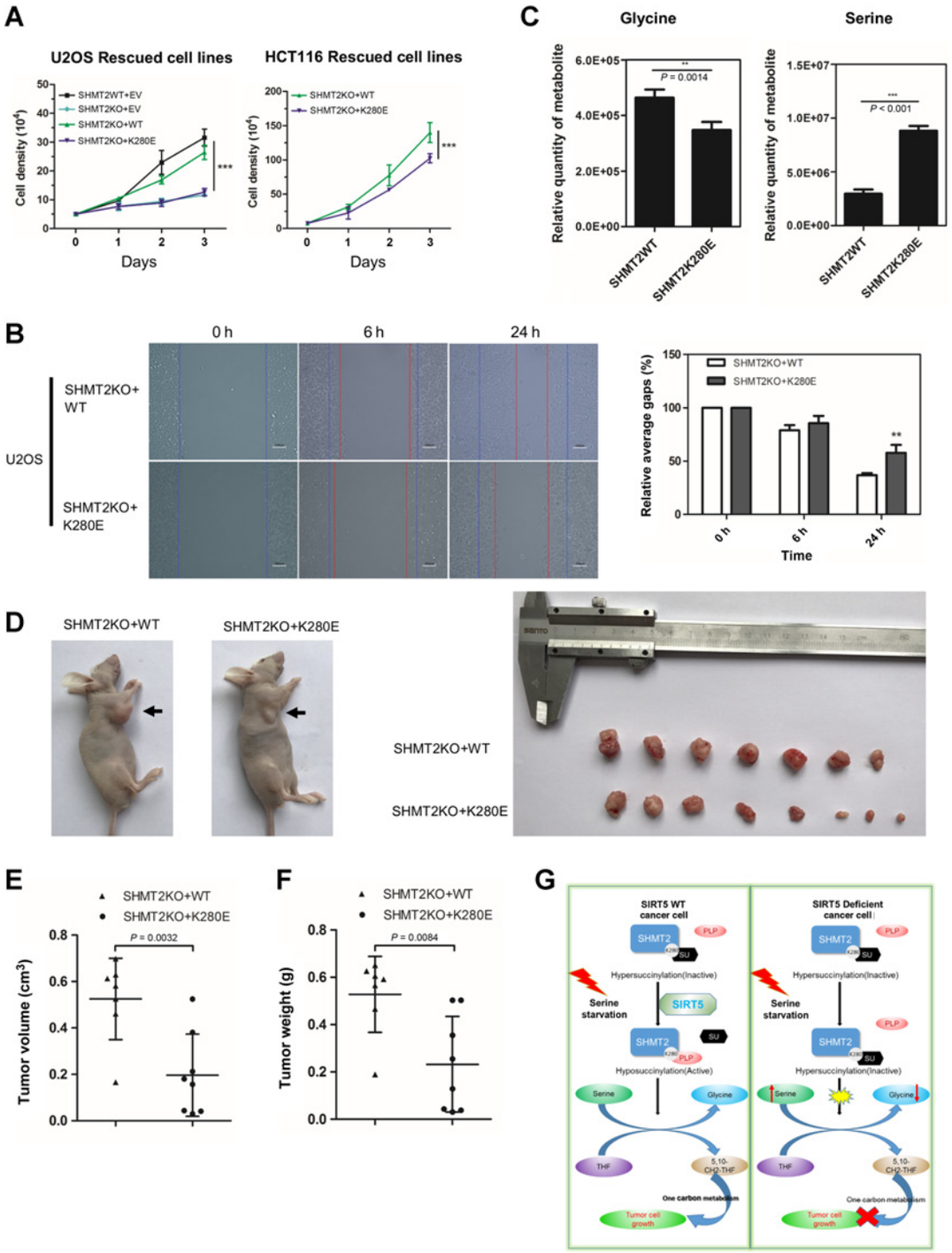

Figure 7.

Succinylation of SHMT2 at K280 impairs tumor cell growth *in vivo* and *in vitro*. **A,** Succinylation of SHMT2 K280 suppresses cell proliferation. U2OS WT cells, SHMT2 KO cells, $SHMT2^{WT}$ cells, or $SHMT2^{K280E}$ cells were seeded into 6-well plates at the same number and treated with or without serine/glycine. Same assay was done by HCT116 $SHMT2^{WT}$ cells or $SHMT2^{K280E}$ cells. Cell numbers were counted every day. Error bars, ±SD ($n = 3$). **B,** SHMT2 WT supports cell migration. U2OS $SHMT2^{WT}$ cells or $SHMT2^{K280E}$ cells were analyzed by wound healing assay. Relative gaps after wound were measured at indicated time point. Error bars, ±SD ($n = 3$). **C,** SHMT2 K280E cells reduced serine catabolism flux. U2OS $SHMT2^{WT}$ cells or $SHMT2^{K280E}$ cells were harvested in 80% confluence in normal medium. Metabolites from cells were analyzed by UPLC–MS/MS. Relative quantity of metabolites is shown (y axis = peak area). Error bars, ±SD ($n = 4$). **D,** SHMT2 K280E impairs tumor growth in a xenograft mouse model. Xenograft was performed in BALB/c nude mice injected with HCT116 $SHMT2^{WT}$ or $SHMT2^{K280E}$ cells described in Supplementary Fig. S7A. Four weeks after injection, mice were sacrificed and tumors were dissected and photographed. **E** and **F,** Quantitation of volume and weight of tumors shown in **D**. Dots represent volume and weight of SHMT2 WT tumors ($n = 7$) or SHMT2 K280E tumors ($n = 8$). Error bars, ±SD. **G,** Model illustrating SHMT2 K280 desuccinylation by SIRT5 regulates cellular redox balance and tumor cell growth.

succinylome and acetylome also overlap in a mass of proteins, such as CS and HSD17B10, which can interact with both SIRT3 and SIRT5 (43). Despite the wide range of overlaps between the interaction network and acylome, specific proteins could have dominant PTM at certain states and in certain cell lines. Our results support this notion.

In general, most of SHMT2 proteins form homodimer in cells without enzymatic activity (2). To activate its activity, SHMT2 goes through a transformation process to form tetramers after binding PLP at the K280 site. This assumption is based on its protein structure. The change of enzymatic activity of SHMT2 K280E also demonstrated that K280 succinylation plays a pivotal role in regulating this process (Fig. 5B). Indeed, SHMT2 K280E showed reduced tetramer formation (Fig. 5D), confirming this notion. In consequence of nonenzymatic catalyst of protein automatic succinylation (41), newly translated SHMT2 may be blocked by succinyl group and maintain its homodimer status without enzymatic activity. When cells are under rapid proliferation state or metabolic stress, SIRT5 desuccinylates SHMT2 and removes the succinyl group from K280 and consequently reinforces the tetrameter formation of SHMT2 to activate its enzymatic activity.

Succinyl-CoA is an active mitochondrial tricarboxylic acid cycle intermediate, and the nonenzymatic reaction by succinyl-CoA is tightly controlled by its concentration in the mitochondria matrix (42). Published proteome shows that SHMT1 is succinylated as well (30), and SHMT1 shares conserved amino acid sequence with SHMT2. In our results, SHMT1 is not shown among the mitochondrial SIRT5-interacted proteins. This could be that we purified SIRT5 complex in mitochondria and SHMT1 is mainly located in cytoplasm.

Glutamic acid is an acidic amino acid that suppresses the binding of enzymes to PLP in comparison with lysine. K280E mimics the succinylation form, which disturbs the tetramer formation of SHMT2 to some extent. In our study, WT-rescued cells showed better resistance to serine/glycine starvation, which was indicated by the $NADPH/NADP^{+}$ ratio, GSH/GSSG ratio, ROS levels, and clonogenic growth (Fig. 6), and K280E-rescued SHMT2 KO cells displayed lower tumor cell growth *in vivo* and *in vitro* than WT-rescued cells (Fig. 7). These results suggest that K280 can be a potential cancer therapy site. SHMT2 is a universal enzyme for cell proliferation and T-cell activation (44). A specific single amino acid mutation technique changing K 280 to E can be used for suppression of SHMT2-related cancer, providing a potential simple tool for cancer therapy.

Our findings on SHMT2 activation positively correlated with SIRT5 desuccinylation under metabolic stress in bone osteosarcoma cells or colon colorectal carcinoma cells, indicating that SIRT5 is a potential oncogene in promoting tumor cell growth. Whether the suppressor or promoter roles are played by SIRT5 in oncogenesis remains to be determined. Recent studies indicate that IDH1-mutant–induced hypersuccinylation impairs mitochondrial functions, and exogenous SIRT5 can decrease the viability of hypersuccinylated tumor cells (33). However, in non–small cell lung cancer, SIRT5 is overexpressed, and increased expression of SIRT5 predicts poor survival (34). Overall, SIRT5 shows different deacylation functions to regulate numerous enzymes that participated among the diverse cellular pathways. Therefore, the function of SIRT5 in tumor development is context dependent. In specific circumstances, the pathway that has been dominantly regulated decided the outcome of tumor suppressor or tumor promoter.

Decreasing intracellular serine and glycine concentration impairs WT HCT116 cell proliferation *in vitro* and *in vivo* (45). SHMT2 K280E mutant, which shows drastically decreasing enzymatic activity, gives less impetus for serine consumption and puts cells under serine/glycine starvation circumstance consequently in another alternative way (Fig. 7C). Thus, SHMT2 K280E results in serine/glycine starvation diet, which reduces tumor growth in xenograft model. Our study demonstrated an important mechanism of SHMT2 regulation by SIRT5 desuccinylation and provided a potential weapon for cancer therapy by targeting the K280 site of SHMT2 (Fig. 7G).

Disclosure of Potential Conflicts of Interest

No potential conflicts of interest were disclosed.

Authors' Contributions

Conception and design: X. Yang, Y. Yin, J. Luo
Development of methodology: X. Yang, Z. Wang, X. Li, B. Liu, J. Luo
Acquisition of data (provided animals, acquired and managed patients, provided facilities, etc.): X. Yang, Z. Wang, X. Li, L. Liu, M. Ren, Y. Wang, M. Yu
Analysis and interpretation of data (e.g., statistical analysis, biostatistics, computational analysis): X. Yang, Z. Wang, X. Li, B. Liu, M. Liu, L. Liu, S. Chen, M. Ren, B. Wang, W.-G. Zhu, J. Luo
Writing, review, and/or revision of the manuscript: X. Yang, B. Liu, M. Liu, L. Liu, S. Chen, W. Gu, J. Luo
Administrative, technical, or material support (i.e., reporting or organizing data, constructing databases): J. Zou
Study supervision: J. Luo

Acknowledgments

We thank Dr. Jiadong Wang (Peking University) for generously providing LentiCRISPRv2 plasmid, Dr. Yingyu Chen (Peking University) for generously providing anti–phospho-S6 and anti-S6 antibodies, and John Luo and Daoyuan Huang for editorial assistance. We thank the core facility at Peking University Health Science Center for mass spectrometry analysis. This work was supported by National Natural Science Foundation of China (81270427, 81471405, 81321003, 81671389) and from National Research Program of China (973 Program, 2013CB530801).

The costs of publication of this article were defrayed in part by the payment of page charges. This article must therefore be hereby marked *advertisement* in accordance with 18 U.S.C. Section 1734 solely to indicate this fact.

Received June 28, 2017; revised October 16, 2017; accepted November 9, 2017; published OnlineFirst November 27, 2017.

References

1. Fu TF, Rife JP, Schirch V. The role of serine hydroxymethyltransferase isozymes in one-carbon metabolism in MCF-7 cells as determined by (13)C NMR. Arch Biochem Biophys 2001;393:42–50.
2. Giardina G, Brunotti P, Fiascarelli A, Cicalini A, Costa MG, Buckle AM, et al. How pyridoxal 5′-phosphate differentially regulates human cytosolic and mitochondrial serine hydroxymethyltransferase oligomeric state. FEBS J 2015;282:1225–41.
3. Kim PB, Nelson JW, Breaker RR. An ancient riboswitch class in bacteria regulates purine biosynthesis and one-carbon metabolism. Mol Cell 2015;57:317–28.

4. Ye J, Fan J, Venneti S, Wan YW, Pawel BR, Zhang J, et al. Serine catabolism regulates mitochondrial redox control during hypoxia. Cancer Discov 2014;4:1406–17.
5. Nikiforov MA, Chandriani S, O'Connell B, Petrenko O, Kotenko I, Beavis A, et al. A functional screen for Myc-responsive genes reveals serine hydroxymethyltransferase, a major source of the one-carbon unit for cell metabolism. Mol Cell Biol 2002;22:5793–800.
6. Kim D, Fiske BP, Birsoy K, Freinkman E, Kami K, Possemato RL, et al. SHMT2 drives glioma cell survival in ischaemia but imposes a dependence on glycine clearance. Nature 2015;520:363–67.
7. Anderson DD, Quintero CM, Stover PJ. Identification of a de novo thymidylate biosynthesis pathway in mammalian mitochondria. Proc Natl Acad Sci U S A 2011;108:15163–8.
8. Jain M, Nilsson R, Sharma S, Madhusudhan N, Kitami T, Souza AL, et al. Metabolite profiling identifies a key role for glycine in rapid cancer cell proliferation. Science 2012;336:1040–4.
9. Labuschagne CF, van den Broek NJ, Mackay GM, Vousden KH, Maddocks OD. Serine, but not glycine, supports one-carbon metabolism and proliferation of cancer cells. Cell Rep 2014;7:1248–58.
10. Chaneton B, Hillmann P, Zheng L, Martin AC, Maddocks OD, Chokkathukalam A, et al. Serine is a natural ligand and allosteric activator of pyruvate kinase M2. Nature 2012;491:458–62.
11. Bao XR, Shao-En O, Olga G, Peng J, Rohit S, Thompson DA, et al. Mitochondrial dysfunction remodels one-carbon metabolism in human cells. Elife 2015;5:pii:e10575.
12. Lewis CA, Parker SJ, Fiske BP, McCloskey D, Gui DY, Green CR, et al. Tracing compartmentalized NADPH metabolism in the cytosol and mitochondria of mammalian cells. Mol Cell 2014;55:253–63.
13. Fan J, Ye J, Kamphorst JJ, Shlomi T, Thompson CB, Rabinowitz JD. Quantitative flux analysis reveals folate-dependent NADPH production. Nature 2014;510:298–302.
14. Maddocks OD, Labuschagne CF, Adams PD, Vousden KH. Serine metabolism supports the methionine cycle and DNA/RNA methylation through De Novo ATP synthesis in cancer cells. Mol Cell 2016;61:210–21.
15. Ben-Sahra I, Hoxhaj G, Ricoult SJ, Asara JM, Manning BD. mTORC1 induces purine synthesis through control of the mitochondrial tetrahydrofolate cycle. Science 2016;351:728–33.
16. DeNicola GM, Chen PH, Mullarky E, Sudderth JA, Hu Z, Wu D, et al. NRF2 regulates serine biosynthesis in non-small cell lung cancer. Nat Genet 2015;47:1475–81.
17. Ding J, Li T, Wang X, Zhao E, Choi JH, Yang L, et al. The histone H3 methyltransferase G9A epigenetically activates the serine-glycine synthesis pathway to sustain cancer cell survival and proliferation. Cell Metab 2013;18:896.
18. Maddocks OD, Berkers CR, Mason SM, Zheng L, Blyth K, Gottlieb E, et al. Serine starvation induces stress and p53-dependent metabolic remodelling in cancer cells. Nature 2013;493:542–6.
19. Ou Y, Wang SJ, Jiang L, Zheng B, Gu W. p53 Protein-mediated regulation of phosphoglycerate dehydrogenase (PHGDH) is crucial for the apoptotic response upon serine starvation. J Biol Chem 2015;290:457–66.
20. Riscal R, Schrepfer E, Arena G, Cisse MY, Bellvert F, Heuillet M, et al. Chromatin-bound MDM2 regulates serine metabolism and redox homeostasis independently of p53. Mol Cell 2016;62:890–902.
21. Yang X, Liu B, Zhu W, Luo J. SIRT5, functions in cellular metabolism with a multiple enzymatic activities. Sci China Life Sci 2015;58:912–4.
22. Polletta L, Vernucci E, Carnevale I, Arcangeli T, Rotili D, Palmerio S, et al. SIRT5 regulation of ammonia-induced autophagy and mitophagy. Autophagy 2015;11:253–70.
23. Tan M, Peng C, Anderson KA, Chhoy P, Xie Z, Dai L, et al. Lysine glutarylation is a protein posttranslational modification regulated by SIRT5. Cell Metab 2014;19:605–17.
24. Nakamura Y, Ogura M, Ogura K, Tanaka D, Inagaki N. SIRT5 deacetylates and activates urate oxidase in liver mitochondria of mice. FEBS Lett 2012;586:4076–81.
25. Nakagawa T, Lomb DJ, Haigis MC, Guarente L. SIRT5 Deacetylates carbamoyl phosphate synthetase 1 and regulates the urea cycle. Cell 2009;137:560–70.
26. Rardin MJ, He W, Nishida Y, Newman JC, Carrico C, Danielson SR, et al. SIRT5 regulates the mitochondrial lysine succinylome and metabolic networks. Cell Metab 2013;18:920–33.
27. Sadhukhan S, Liu X, Ryu D, Nelson OD, Stupinski JA, Li Z, et al. Metabolomics-assisted proteomics identifies succinylation and SIRT5 as important regulators of cardiac function. Proc Natl Acad Sci U S A 2016;113:4320–5.
28. Colak G, Pougovkina O, Dai L, Tan M, Te BH, Huang H, et al. Proteomic and biochemical studies of lysine malonylation suggest its malonic aciduria-associated regulatory role in mitochondrial function and fatty acid oxidation. Mol Cell Proteomics 2015;14:3056–71.
29. Nishida Y, Rardin MJ, Carrico C, He W, Sahu AK, Gut P, et al. SIRT5 regulates both cytosolic and mitochondrial protein malonylation with glycolysis as a major target. Mol Cell 2015;59:321–32.
30. Park J, Chen Y, Tishkoff DX, Peng C, Tan M, Dai L, et al. SIRT5-mediated lysine desuccinylation impacts diverse metabolic pathways. Mol Cell 2013;50:919–30.
31. Zhou L, Wang F, Sun R, Chen X, Zhang M, Xu Q, et al. SIRT5 promotes IDH2 desuccinylation and G6PD deglutarylation to enhance cellular antioxidant defense. EMBO Rep 2016;17:811–22.
32. Lin ZF, Xu HB, Wang JY, Lin Q, Ruan Z, Liu FB, et al. SIRT5 desuccinylates and activates SOD1 to eliminate ROS. Biochem Biophys Res Commun 2013;441:191–5.
33. Li F, He X, Ye D, Lin Y, Yu H, Yao C, et al. NADP(+)-IDH mutations promote hypersuccinylation that impairs mitochondria respiration and induces apoptosis resistance. Mol Cell 2015;60:661–75.
34. Lu W, Zuo Y, Feng Y, Zhang M. SIRT5 facilitates cancer cell growth and drug resistance in non-small cell lung cancer. Tumour Biol 2014;35:10699–705.
35. Wei F, Luo J. SIRT1 regulates UV-induced DNA repair through deacetylating XPA. Mol Cell 2010;39:247.
36. Wieckowski MR, Giorgi C, Lebiedzinska M, Duszynski J, Pinton P. Isolation of mitochondria-associated membranes and mitochondria from animal tissues and cells. Nat Protoc 2009;4:1582–90.
37. Shin M, Bryant JD, Momb J, Appling DR. Mitochondrial MTHFD2L is a dual redox cofactor-specific methylenetetrahydrofolate dehydrogenase/methenyltetrahydrofolate cyclohydrolase expressed in both adult and embryonic tissues. J Biol Chem 2014;289:15507–17.
38. Zhou J, Liu H, Liu Y, Liu J, Zhao X, Yin Y. Development and evaluation of a parallel reaction monitoring strategy for large-scale targeted metabolomics quantification. Anal Chem 2016;88:4478–86.
39. Ran FA, Hsu PD, Wright J, Agarwala V, Scott DA, Zhang F. Genome engineering using the CRISPR-Cas9 system. Nat Protoc 2013;8:2281–308.
40. Krall AS, Xu S, Graeber TG, Braas D, Christofk HR. Asparagine promotes cancer cell proliferation through use as an amino acid exchange factor. Nat Commun 2016;7:11457.
41. Wagner GR, Payne RM. Widespread and enzyme-independent Nepsilon-acetylation and Nepsilon-succinylation of proteins in the chemical conditions of the mitochondrial matrix. J Biol Chem 2013;288:29036–45.
42. Wagner GR, Bhatt DP, O'Connell TM, Thompson JW, Dubois LG, Backos DS, et al. A class of reactive Acyl-CoA species reveals the non-enzymatic origins of protein acylation. Cell Metab 2017;25:823.
43. Yang W, Nagasawa K, Münch C, Xu Y, Satterstrom K, Jeong S, et al. Mitochondrial sirtuin network reveals dynamic SIRT3-dependent deacetylation in response to membrane depolarization. Cell 2016;167:985–1000.
44. Ron-Harel N, Santos D, Ghergurovich JM, Sage PT, Reddy A, Lovitch SB, et al. Mitochondrial biogenesis and proteome remodeling promote one-carbon metabolism for T cell activation. Cell Metab 2016;24:104–17.
45. Odk M, Athineos D, Cheung EC, Lee P, Zhang T, Njf VDB, et al. Modulating the therapeutic response of tumours to dietary serine and glycine starvation. Nature 2017;544:372.